Flood forecasting in the Tiber catchment area: a methodological analysis

Guido Calenda ([1]), **Marco Casaioli** ([2]), **Claudio Cosentino** ([1]), **Roberta Mantovani** ([3]) and **Antonio Speranza** ([4])([5])

([1]) *Università di «Roma Tre», Dipartimento di Scienze dell'Ingegneria Civile, Roma, Italy*

([2]) *CNR, Istituto di Fisica dell'Atmosfera, Roma, Italy*

([3]) *Università di Bologna, Dipartimento di Fisica, Bologna, Italy*

([4]) *Università di Camerino, Dipartimento di Matematica e Fisica, Camerino, Italy*

([5]) *Presidenza del Consiglio dei Ministri, Dipartimento dei Servizi Tecnici Nazionali, Roma, Italy*

Abstract

The most difficult step in hydrological forecasting is precipitation forecast, since rain is the most irregular and least predictable meteorological field. Numerical meteorological models are the main tool to forecast the precipitation field over river basins where floods may be expected. Object of this paper is a preliminary analysis of the appropriate methodological approach to flood forecasting in the Tiber River basin. An assessment of the flood forecasting skill of a meteorological limited area model, coupled with a lumped rainfall-runoff model, is performed. The main indications which seem to arise are that integral precipitation over the catchment area is adequately forecast in its time-evolution, but the total rainfall shows a systematic deficit with respect to observations.

Key words *precipitation – flood – forecast – LAM – runoff modelling*

1. Introduction

Object of this paper is the preliminary analysis of numerical flood forecast in the basin of the Tiber River, limited to the gauging site of Ponte Nuovo. The basin (shown in fig. 1) is located in Central Italy, covers an area of 4147 km^2, is mostly impermeable (84%) and is characterised by a lag-time of 18-22 h. Our choice of this basin is due essentially to three factors:

– Its phenomenology of intense precipitation is relatively simple with respect to other Mediterranean areas: it is basically associated with humid frontal advection from the Tyrrenian Sea and condensation due to orographic uplift in the Tiber basin.

– The basin is large enough to be approximately resolved by the standard numerical grids of presently available meteorological models.

– The observational coverage is adequate for our purposes of preliminary assessment of numerical flood forecast.

The downscaling sequence we analyse starts from gridded global meteorological fields released by the European Centre for Medium-Range Weather Forecasts (ECMWF) and produces a forecast of Mediterranean scale precipitation fields by means of a Limited Area Model

Mailing address: Prof. Antonio Speranza, Presidenza del Consiglio dei Ministri, Dipartimento dei Servizi Tecnici Nazionali, Via Curtatone 3, 00185 Roma, Italy; e-mail: antonio.speranza@dstn.it

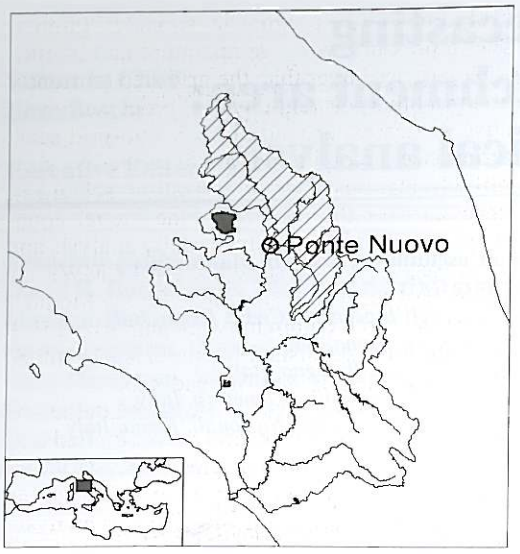

Fig. 1. Tiber basin and Ponte Nuovo rain-gauge station: the shaded region refers to the river watershed selected for the study and the insert shows the location within the Mediterranean area.

(LAM); the gridded precipitation field over the Tiber basin is used as input for a hydrological model of runoff in the Tiber River.

In Section 2 we describe the hydrometeorological phenomenology and the adopted forecast approach; in Section 3 we discuss the selected case studies; in Section 4 we draw our conclusions.

2. Phenomenology of intense precipitation and flooding in the Tiber River basin and adopted forecast approach

It is a well known property of Mediterranean precipitation to follow, on average, orographic slope contours. In fact the «Mediterranean air» used to be considered in classical synoptic meteorology (see, for example, U.K. Meteorological Office, 1962) a prototype of «metastable air»: air in which infinitesimal vertical displacements generally do not trigger vertical overturning and consequent precipitation, while finite amplitude vertical displacements – typically associated with orographic uplift – determine strong vertical overturning and precipitation. The primary input of atmospheric precipitable water is humid advection associated with synoptic scale perturbations entering the Mediterranean area from the Atlantic. Cyclonic and frontal activity, however, is influenced by orographic and diabatic (in particular, the release of latent and sensible heat by the Mediterranean Sea) effects. In fact, as soon as specific hydrometeorological events are analysed, it clearly appears that water in the Mediterranean atmosphere is characterised by many space-time aggregation scales: from the frontal scale of the Atlantic cold intrusions, to the sub-frontal scale of features associated with frontal interaction with orography, down to the very small scale of local convective events like, for example, the one associated with the Versilia flooding of 1996.

In the quite complex context indicated above, the phenomenology of intense precipitation and flooding in the Tiber basin appears relatively simple. From systematic examination of the past record of events, frontal and orographic processes seem to be dominant: humid south-westerly winds, associated with fronts running more or less orthogonally to the Tyrrhenian coast, enter the Tiber valley and blow over the local mountains, forcing an orographic uplift of humid air.

Flood-flow formation in the Tiber River (at Ponte Nuovo) is the consequence of the additive effects of flood-peaks coming from the upper reach and from the main tributary – the Chiascio River – which joins the Tiber just upstream of the gauging site. Due to the virtual absence of snow deposits and major lakes (*) and to the moderate extension of pervious area (about 16% of the basin), flow modulation is mainly exerted by the widespread flooding of the valleys. Rainfall events covering the entire basin and lasting at least 1-2 days appear to be the main forcing factors in the development of flood-flows. An-

(*) In the past the only artificial impoundment on the Tiber River was the Corbara reservoir, downstream of Ponte Nuovo. Now two artificial reservoirs are becoming operational, one on the upper Tiber and the other on the Chiascio River.

other key factor is the saturation of the basin soil, usually due to previous precipitation.

The precipitation inputs for classical hydrological flood-forecasting models consist in real-time observations at available rain-gauges: rainfall, as estimated from interpolation of observations, is used as forcing in the river flow model. This procedure is not optimal for forecasting purposes in small basins, where the time-scale of response to intense precipitation is of the order of a few hours. In such conditions, the obvious advantage of using a meteorological numerical model is that it can provide a rainfall forecast one or more days in advance.

The output of a numerical meteorological model is discretised over a regularly spaced grid and the grid-point values of the water depth represent the average value of the variable over the associated grid-box: the larger is the number of grid-points falling in the basin, the more accurate can be the representation.

The basin of the Tiber River is wide enough to contain several grid-points, but it is also characterised by a lag-time small enough to make numerical forecasting potentially beneficial for purposes of early forecast.

Objective of our research is a preliminary test of numerical flood forecast for operational purposes. ECMWF and LAM precipitation forecasts are compared with observed precipitation; LAM precipitation is coupled with a lumped hydrological rainfall-runoff model and the results are compared with those obtained by forcing the same hydrological model with precipitation observed at rain-gauges.

The ECMWF meteorological model is a global, spectral, primitive equation model, *i.e.* it solves over the whole globe the equations of atmospheric dynamics and thermodynamics projected on a truncated series of spherical harmonics. Initial conditions are provided to the model by a global description of the observed state of the atmosphere over a regular grid (analysis) which is also produced by ECMWF. In order to produce analysis, ECMWF collects many existing observations (land-based, rawinsondes, ships, planes and satellites) in real-time and, by means of a sophisticated algorithm performs the assimilation of the observation over the grid. As the primitive equations describe only the time evolution of the prognostic variables (atmospheric pressure, wind, temperature and humidity) on scales larger than the grid step (currently 50 km), other relevant physical processes (radiative processes, ground physics, sub-grid scale turbulence, precipitation) are described by simplified relations (parameterization schemes), necessary for the closure of the model equations. The ECMWF produces daily analysis and forecasts, which are stored in the ECMWF archive. Past records are available for the Member States' research community; an authorized FTP procedure is established for the data download (for further details, see Appendix I).

A LAM differs from a global model as the integration domain is restricted to a limited area so that, besides initial conditions, boundary conditions are needed throughout the run. In our case, these are provided by ECMWF analysis. The model is a version of BOLAM (BOlogna LAM; see Buzzi *et al.*, 1994); incorporating a parameterization scheme for convective precipitation developed by Emanuel (1991). The model horizontal resolution is about 27 km and the integration domain covers approximately the Central Mediterranean area (for further details, see Appendix I).

The hydrological model used in this study (see Appendix II for details) is a deterministic lumped model based on a very simplified representation of the physical processes of flood formation at the catchment level: although a physical meaning can be assigned to the parameters included in the model equations, a calibration procedure is nonetheless required to set-up the model.

Basically the model includes three modules:

– A *base flow module*, setting the subsurface contributions.

– A *hydrological losses module*, computing hydrological losses due to evapotranspiration, interception, depression storage and infiltration: the remaining «Excess Rainfall Hyetograph» (ERH) represents the amount of water actually contributing to the river flood.

– A *flow concentration module*, generating the «Direct Runoff Hydrograph» (DRH) from the ERH; this module reproduces the transfer and concentration of surface water through catchment slopes and river channels.

In the first module the base-flow is set equal to the minimum discharge occurring just before the beginning of the rising limb of the hydrograph. This schematic representation is based on the assumption that the flood events are due to intense and short duration rainfall storms: therefore direct overland flow exceeds the other flow contributions, especially for an impermeable basin.

The second module consists in a double-threshold device, triggering the selection of the runoff coefficient. When the precipitation depth exceeds a given threshold value, a larger coefficient is employed. This mechanism simulates the increase in excess precipitation as soil moisture increases. In order to account for the initial soil moisture, the precipitation depth at the beginning of the event is set equal to the total rain fallen in the five preceding days.

The third module consists in a unit hydrograph based on the «multiple linear reservoirs scheme» (Nash, 1957).

The overall parameter set includes 5 parameters for the first module and 2 for the second. Input to the model are the time series of rain depths averaged over the river watershed.

The watershed is simply sketched as a single operator transforming the spatially averaged rainfall depth over the basin into flood flow. The spatial inhomogeneities of the rain field and the spatial features of the watershed are lumped into the model equations and parameters.

3. Case studies

The selected river watershed is characterized by a catchment area being covered by 9 boxes (centered on the grid-points) of the ECMWF grid (fig. 2a) and 13 of the LAM grid (fig. 2b). Moreover, a considerable number of rain-gauges are available in the area: observations from 16 of them have been used in our study.

Thirty-hour and fifty-four-hour forecasts were performed. Since precipitation is not an initialised field, the first six hours of the forecast were

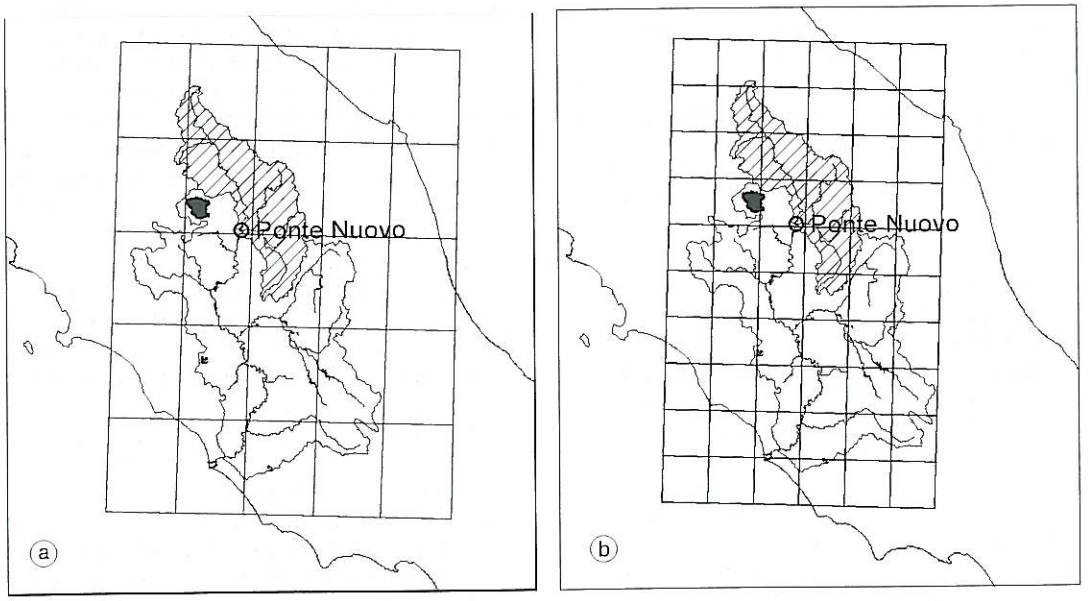

Fig. 2a,b. Numerical grid projections onto the Tiber basin: a) ECMWF grid; b) LAM grid. The shaded region refers to the river watershed selected for the study.

not considered in order to allow the model to develop numerical precipitation from initial precipitable water in the model atmosphere.

All rainfall events that produced significant floods at Ponte Nuovo in the last decade were initially considered. For the purposes of this preliminary investigation, four events among the most intense ones were selected as representative of two typical categories: «long events», displaying two flood-maxima, with a duration of several days each; «short events», displaying a single maximum not longer than one day. The selected cases are:

– Long events: Case 1, December 5-9, 1992; Case 2, December 23-27, 1993.

– Short events: Case 3, January 4-5, 1994; Case 4, December 13-14, 1996.

3.1. *Observed and numerically forecast precipitation*

The LAM precipitation forecasts were compared with the analogous ECMWF forecasts and with direct rain-gauge observations. Notice that this comparison is not meant to assess the quality of the model forecast since, given the irregular structure of the precipitation field, it is quite difficult to assess the accuracy of an estimate of the total precipitation over the basin area obtained by interpolating discrete observations. The purpose of this comparison is mainly to evaluate the consistency of rain values obtained by different sources in a forecast framework.

The estimate of the mean areal rainfall from rain-gauge observations was performed by the Thiessen method.

Since ECMWF precipitation forecasts for less than 6 h intervals were not available, the comparison with the ECMWF forecast was performed only for the 6 h cumulated precipitation.

The LAM forecasts, instead, were also compared with rain-gauge observations for shorter intervals: 3 h for the long events, 1 h for the short events. Precipitation cumulated on the same intervals was used as input for the hydrological model.

The following indexes were introduced to evaluate the performance of the meteorological model in reproducing the observed patterns (for long events, the indexes refer to the single semi-events):

– Total Depth (TD).

– Peak Intensity (PI).

– Shape Error (SE), obtained by shifting in time the forecast precipitation series so that the maximum precipitation time coincides with the observed one and then calculating the root total square error of the observation with respect to the «shifted» forecast, as a percentage of TD

$$SE = \frac{1}{TD}\sqrt{\sum_i (p_i^o - p_i^s)^2}$$

where p_i^s is the «shifted» forecast series and p_i^o is the observed one.

3.2. *Flood-discharge forecast procedure*

Flood forecasts were performed with warning times of 24 and 48 h, after eliminating, as already said, the first 6 h of each forecast.

Due to the inhomogeneity of the rain fields, the estimates of precipitation cumulated over discrete time intervals and averaged on the watershed area, obtained from rain-gauge measurements or from meteorological forecasts, are expected to differ significantly. This greatly affects the hydrological model calibration phase. Model parameters incorporate, among others, the errors in rain depth evaluation. Therefore, the parameters obtained from the calibration based on point observations may prove non-homogeneous with respect to the input values stemming from other sources.

In this preliminary study the areal precipitation estimated from the rain-gauges observations was assumed to represent the «true» rain distribution. Therefore the parameters of the hydrological model were estimated off-line using the rain-gauge observations. The parameter estimation was performed in three steps:

– Preliminary calibration on the 1992 and 1994 events.

– Verification on the 1993 and 1996 events.
– Final calibration on all the events.

The calibration was performed by automatic minimisation of an objective-function F given by the mean square error between forecast and observed flows. Such a function weights more the high flow errors, thus yielding the best parameters for forecasting peak-flows, that are the most prominent features in flood warning.

Using the calibrated model, the following forecasts were performed:

– Forecast 1: at the initial time $t = 0$ a precipitation forecast is issued and the hydrological model is run in the forecasting mode. After each 24 h period a new meteorological forecast is issued up to the end of the event. The hydrological model is run from $t = 0$ every 24 h, using LAM precipitation forecasts.

– Forecast 2: same as above, but the hydrological model is run using the LAM precipitation forecasts for the last 24 h of the flood forecast and the rain-gauge observations for the preceding hours.

– Forecast 3: same as in forecast 2, but with 48-h forecasts.

3.3. *Synoptic description of selected events*

Case 1: December 5-9, 1992 – Two synoptic scale perturbations pass in sequence over the Mediterranean, each one causing intense precipitation. Local cyclogenesis occurs in both cases (fig. 3a,c). As can be seen in fig. 3b, in the first sub-event precipitation occurs when the perturbation runs over land, where the frontal uplift is coupled with the orographic uplift in producing the precipitation event. For the second sub-event (fig. 3d) the interpretation is more difficult because a band of precipitation develops and precipitation can take place even in the absence of orographic uplift. The associated flood event, lasting five days, is characterized by two peaks of equal intensity. The peak discharge of this flood is the maximum flow recorded in the last ten years at Ponte Nuovo.

Case 2: December 23-27, 1993 – As in Case 1, the meteorological event includes two synoptic perturbations associated with intense precipitation. For the first sub-event frontal and orographic uplift operate jointly in producing precipitation; the second one, instead, is associated with a wide frontal precipitation area over the Tyrrenian Sea and, again, precipitation can take place even in the absence of orographic uplift; this fact is not in contrast with a possible strengthening induced by orographic uplift.

Case 3: January 4-5, 1994 – The event seems to be dominated by mesoscale processes. Though a pressure trough is present aloft, the surface pattern is more complex, with several fronts and pressure lows. Numerical precipitation does not occur in the frontal areas, but at the impact of a well organised south-westerly wind with the orographic system. The associated flood develops in only 12 h. Since the rainfall is not very intense, the flood is probably due to soil saturation caused by persistent precipitation in the preceding week.

Case 4: December 13-14, 1996 – The synoptic scenario is characterised by a pressure trough, both at the surface (fig. 4a) and aloft (not shown). Again, precipitation occurs when the frontal structure reaches the orographic slope (fig. 4b), the wind being south-westerly. The associated flood event, lasting 24 h, has the same characteristics as the 1994 event.

3.4. *Forecasts*

Comparison of forecast with observed floods is reported below for the different events.

Case 1: December 5-9, 1992 – As shown in fig. 5a, both the ECMWF and LAM models reproduce the main features of the event, correctly timing the precipitation maxima. Both models, however, systematically underestimate the total precipitation volumes as reconstructed from precipitation measured by rain-gauges (TD in table I). The underestimate is especially relevant in the first sub-event. Although the LAM precipitation depth estimate is worse than the ECMWF one, the LAM better reproduces the time pattern of the precipitation field, also at enhanced time resolution (fig. 5b). Furthermore,

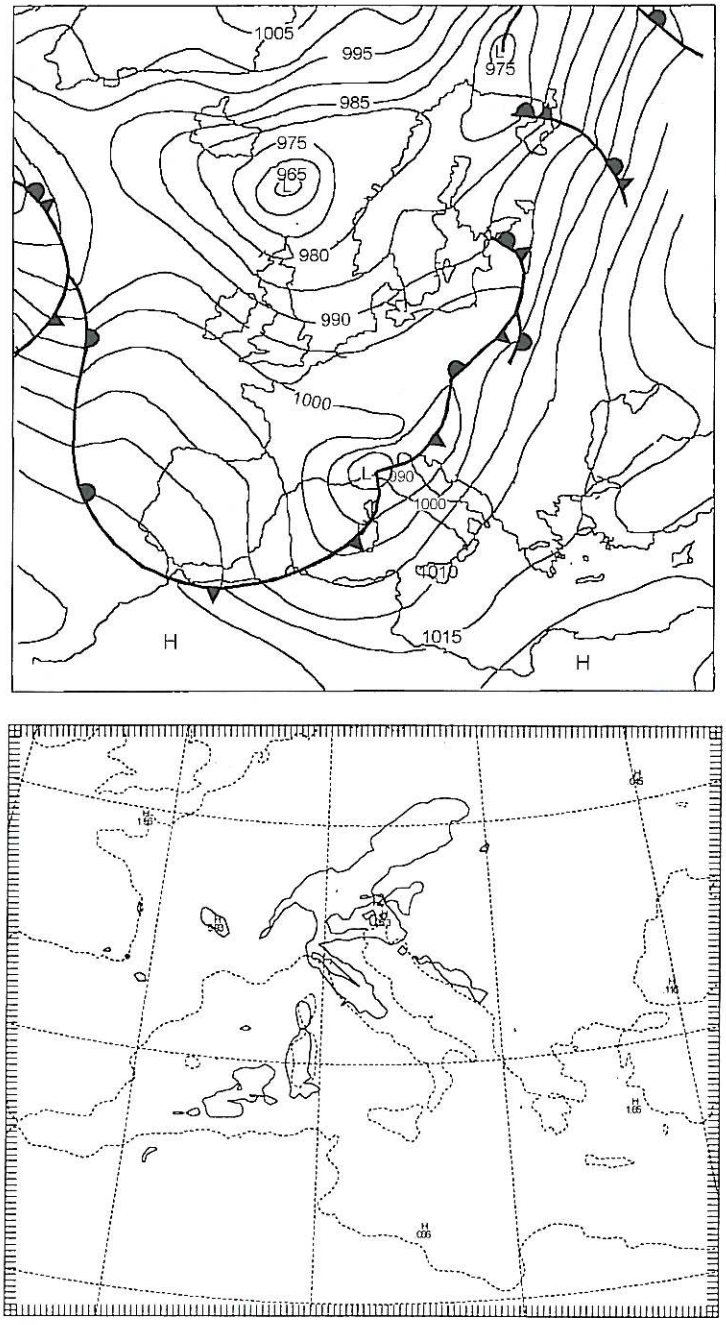

Fig. 3a,b. Case 1, December 1992: a) surface pressure field analysis for December 5, 1992 at 12:00; b) LAM precipitation forecast for December 5, 1992 at 12:00.

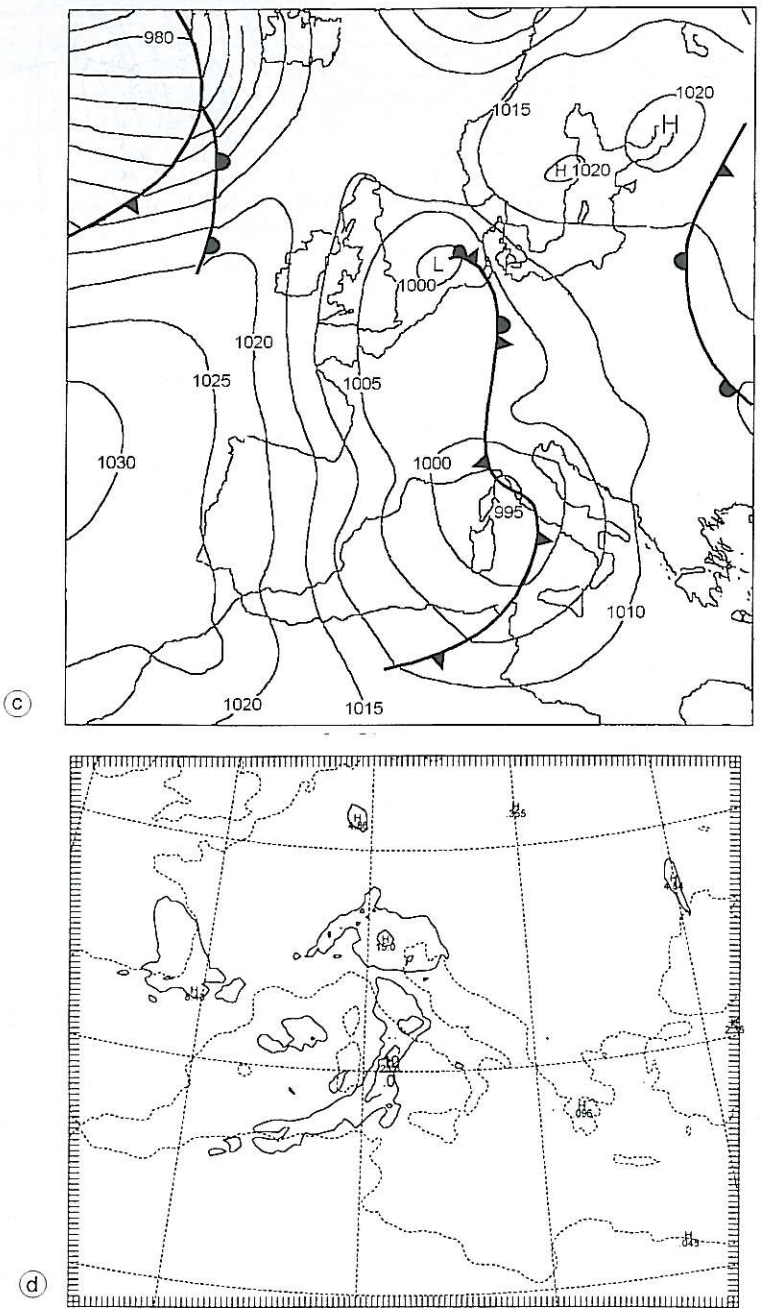

Fig. 3c,d. Case 1, December 1992: c) as in fig. 3a, but for December 8, 1992 at 00:00; d) as in fig. 3b, but for December 8, 1992 at 00:00.

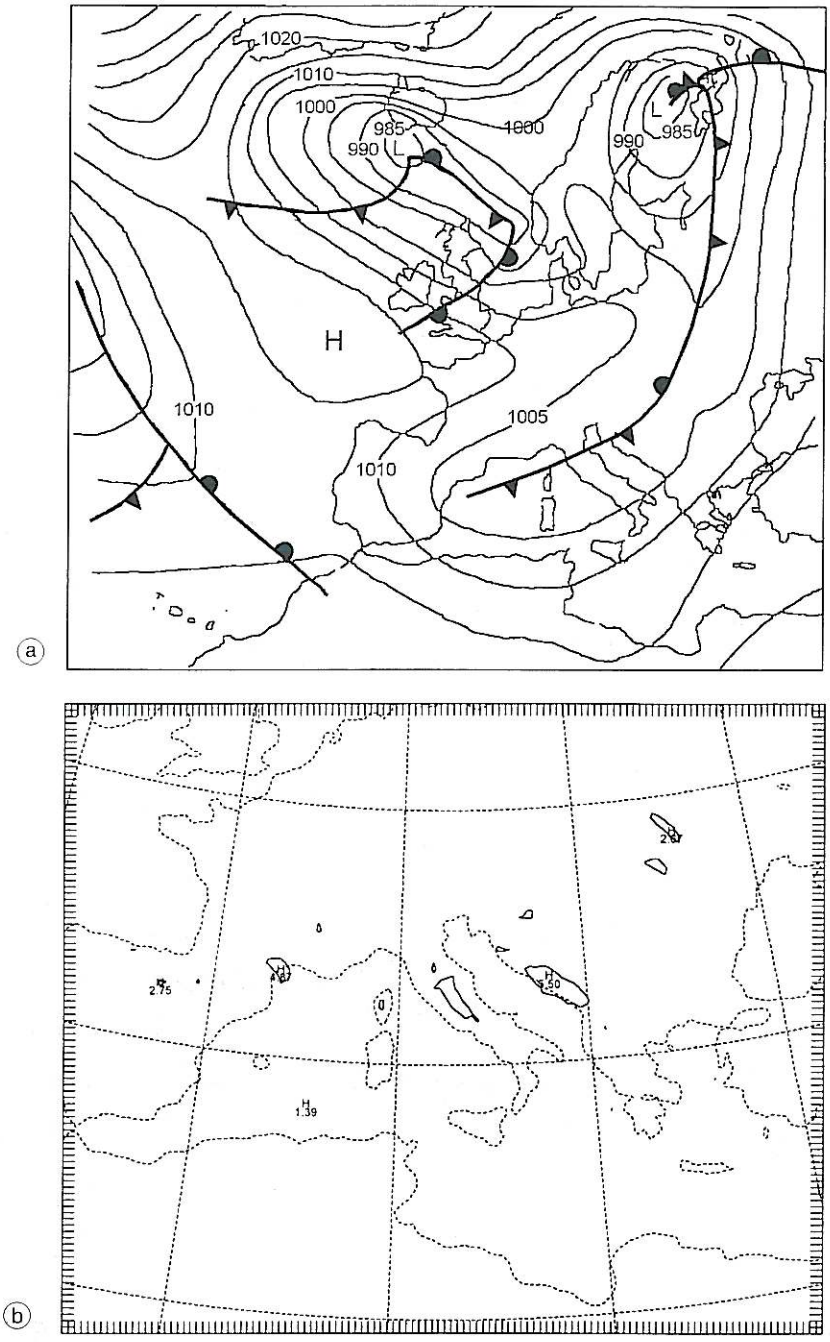

Fig. 4a,b. Case 4, December 1996: a) surface pressure field analysis for December 14, 1996 at 12:00; b) LAM precipitation forecast for December 14, 1996 at 12:00.

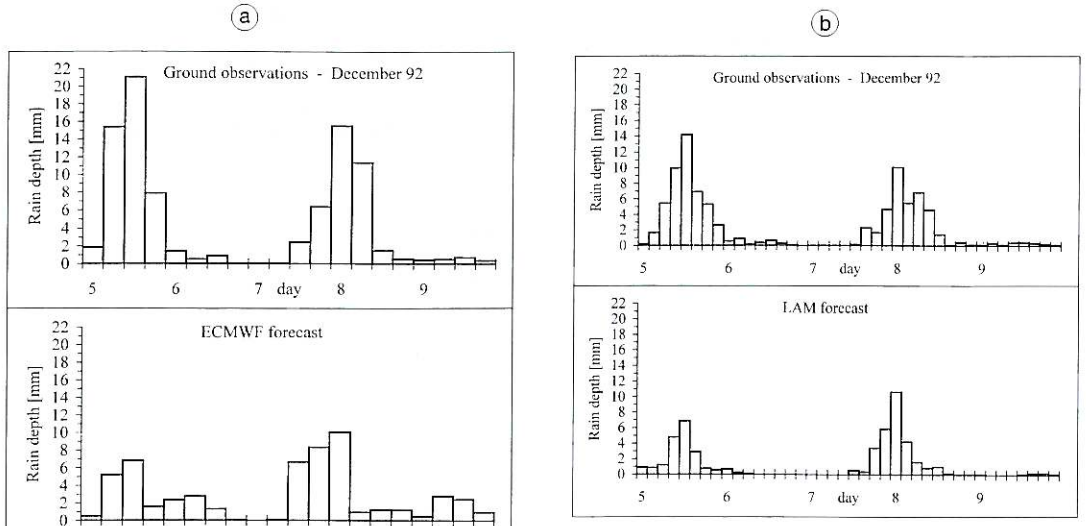

Fig. 5a,b. Case 1, December 1992. Comparison of hyetographs: a) 6-h cumulated rainfall as computed from point observations, from ECMWF 24-h forecast and from LAM 24-h forecast; b) 3-h cumulated rainfall from point observations and from LAM 24-h forecast.

Table I. Case 1, December 1992: comparison of performance indexes of ECMWF and LAM model forecasts. TD is the Total Depth, TD_{Ratio} is $TD_{observation}/TD_{forecast}$, PI is the Peak Intensity, PI_{Ratio} is $PI_{observation}/PI_{forecast}$, SE is the Shape Error; each index refers to the single sub-event. Number 1 refers to the first sub-event (start 5 December 00.00, end 6 December 24.00); number 2 refers to the second sub-event (start 7 December 00.00, end 9 December 24.00). The asterisk indicates the same value as in the respective 6-h case.

December 1992	Sub-event	TD (mm)	TD_{Ratio}	PI (mm)	PI_{Ratio}	SE
Obs. - 6 h	1	43.7	–	21.1	–	–
	2	40.1	–	15.5	–	–
ECMWF	1	20.6	0.471	6.8	0.324	3.716
	2	35.1	0.877	10.0	0.647	3.777
LAM - 6 h	1	18.6	0.425	9.8	0.464	2.110
	2	29.4	0.734	14.9	0.960	3.298
Obs. - 3 h	1	*	–	14.2	–	–
	2	*	–	10.0	–	–
LAM - 3 h	1	*	*	6.9	0.485	1.301
	2	*	*	10.6	1.060	1.795

as shown in table I, the LAM Shape Error is smaller than the ECMWF one, becoming even smaller as the time resolution increases and the peak values are better evaluated by the LAM at both time resolutions.

Although the general time pattern of the flood is essentially captured, forecasts 1 (fig. 6a) and 3 (not shown) are completely unsatisfactory in terms of flood volume and peak values. Forecast 2 (fig. 6b) shows a better agreement espe-

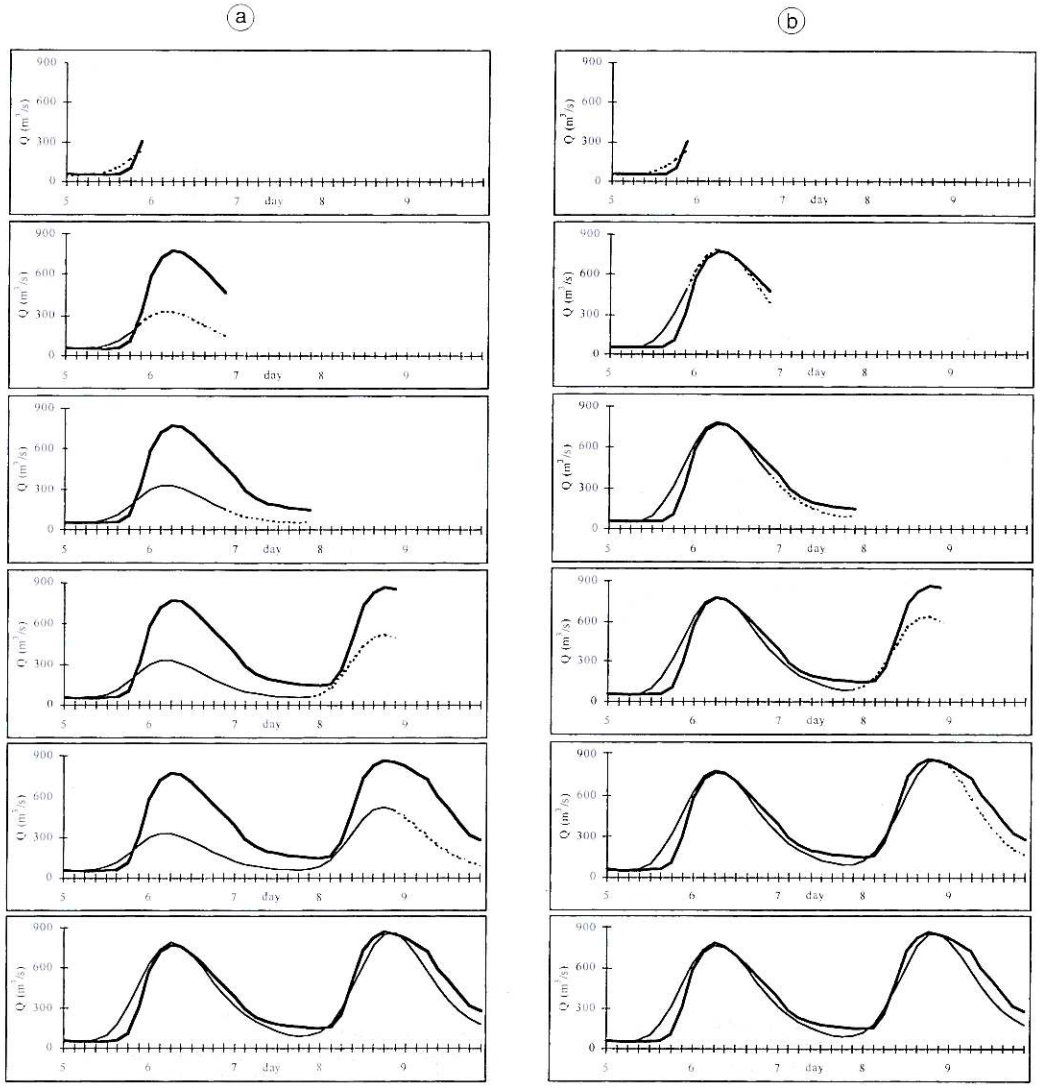

Fig. 6a,b. Case 1, December 1992. Flood forecasting sequence: a) forecast 1, 24-h forecast using LAM rainfall forecast from the beginning of the event; b) forecast 2, 24-h forecast using LAM rainfall forecast only for the last 24 h. Thick line refers to the observed flow, thin line refers to the first part of the forecast and dotted line refers to the second part of the forecast (last 24 h). The last hydrograph represents the comparison between observed (thick line) and modelled (thin line) flood flows using calibration rainfall data as input to the hydrological model.

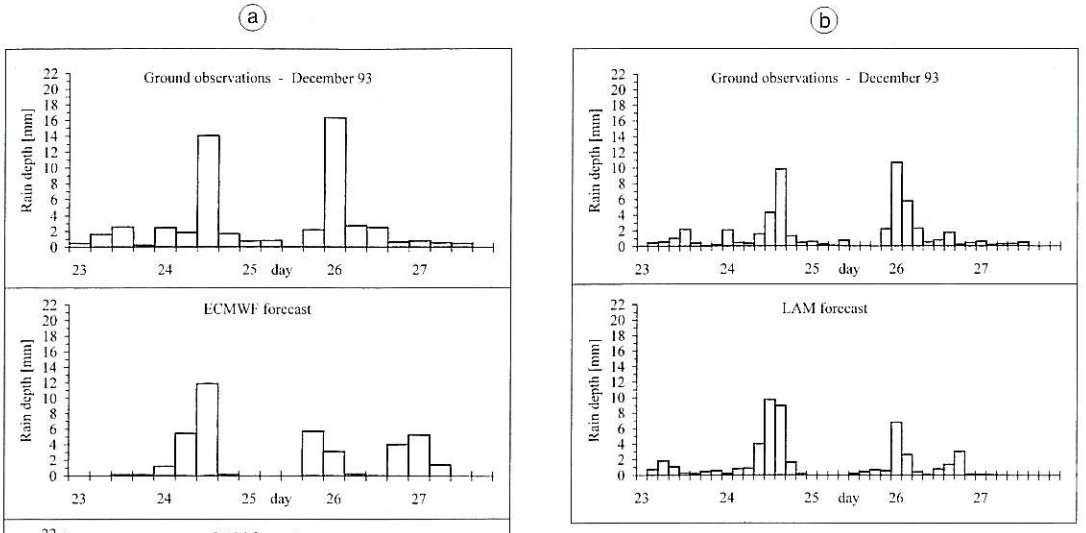

Fig. 7a,b. As fig. 5a,b, but for Case 2, December 1993.

Table II. As table I, but for Case 2, December 1993. Number 1 refers to the first sub-event (start 23 December 18.00, end 25 December 18.00); number 2 refers to the second sub-event (start 25 December 18.00, end 27 December 18.00).

December 1993	Sub-event	TD (mm)	TD_{Ratio}	PI (mm)	PI_{Ratio}	SE
Obs. - 6 h	1	21.9	–	14.0	–	–
	2	26.3	–	16.4	–	–
ECMWF	1	18.8	0.861	11.9	0.846	1.869
	2	19.8	0.753	5.7	0.349	3.911
LAM - 6 h	1	27.4	1.254	18.6	1.326	1.129
	2	17.4	0.663	9.4	0.575	1.694
Obs. - 3 h	1	*	–	9.8	–	–
	2	*	–	10.6	–	–
LAM - 3 h	1	*	*	9.7	0.992	1.719
	2	*	*	6.8	0.638	1.205

cially in forecasting the first peak. This is mainly due to the basin time-response, which is about 20 h: the peak value results from the contributions of the rain fallen 20 h before, which is the observed rain (not the forecast one).

Case 2: December 23-27, 1993 – As shown in fig. 7a,b, the LAM more accurately forecasts the time structure of the precipitation event: the ECMWF forecast (fig. 7a) gives a particularly poor representation of the second sub-event (SE in table II). However, the LAM prediction of the total depth is still worse than the ECMWF one, since it overestimates the first sub-event and strongly underestimates the second one.

Forecasts 1 (fig. 8a) and 3 (not shown) overestimate the first flood peak and underestimate the second one, due to the corresponding errors in the rainfall forecast. Forecast 2 (fig. 8b) seems more successful. This is again explained by the fact that the rain determining the flood peak has already fallen at the beginning of the forecast period.

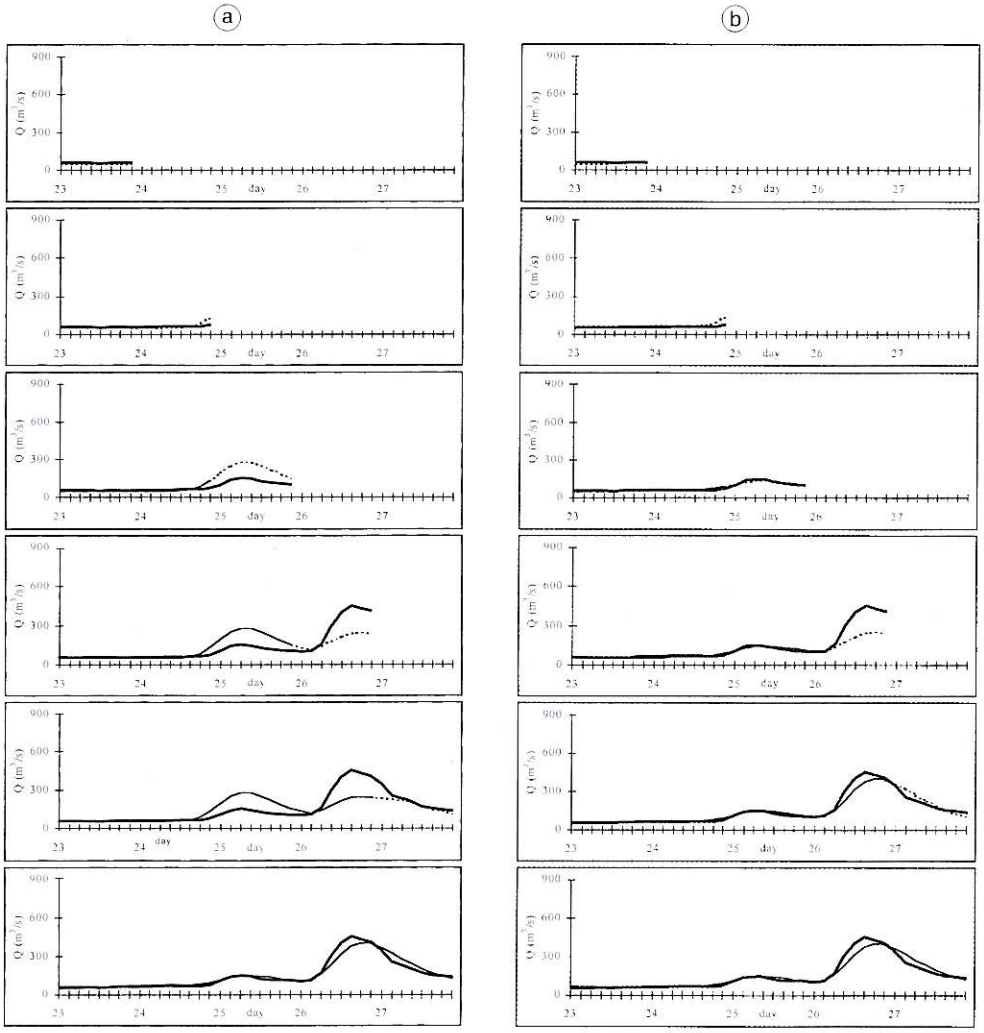

Fig. 8a,b. As fig. 6a,b, but for Case 2, December 1993.

Case 3: January 4-5, 1994 – As shown in fig. 9a, both models give a poor description of the event structure; this is not surprising, due to the modest amplitude of the meteorological perturbation and the absence of a well defined hydrometeorological situation. The description of the phenomenon given by the LAM is somewhat better, particularly if the time resolution is increased (fig. 9b and table III). This improvement may be explained by the better LAM ability to simulate the sub-synoptic scale processes.

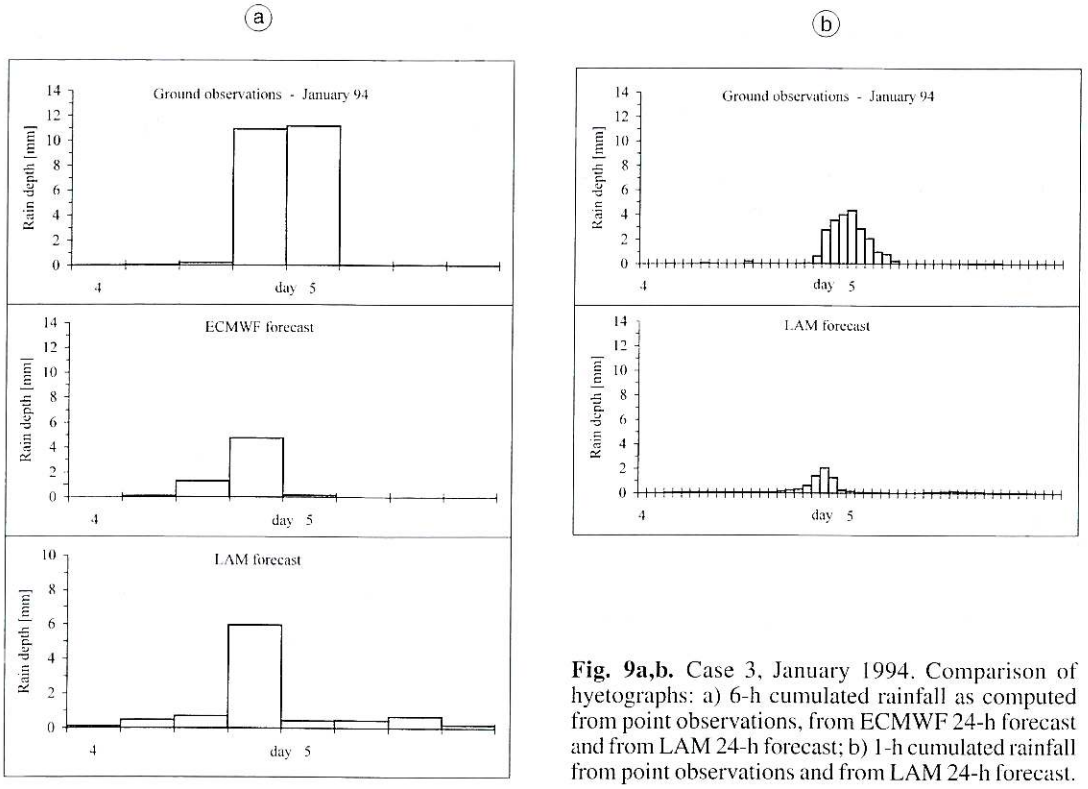

Fig. 9a,b. Case 3, January 1994. Comparison of hyetographs: a) 6-h cumulated rainfall as computed from point observations, from ECMWF 24-h forecast and from LAM 24-h forecast; b) 1-h cumulated rainfall from point observations and from LAM 24-h forecast.

Table III. Case 3, January 1994: comparison of performance indexes of ECMWF and LAM model forecasts. TD is the Total Depth, TD_{Ratio} is $TD_{observation}/TD_{forecast}$, PI is the Peak Intensity, PI_{Ratio} is $PI_{observation}/PI_{forecast}$, SE the Shape Error. The asterisk indicates the same value as in the respective 6-h case.

January 1994	TD (mm)	TD_{Ratio}	PI (mm)	PI_{Ratio}	SE
Obs. - 6 h	22.4	–	11.2	–	–
ECMWF	6.3	0.283	4.7	0.425	5.729
LAM - 6 h	8.0	0.356	5.9	0.533	5.279
Obs. - 1 h	*	–	4.3	–	–
LAM - 1 h	*	*	2.1	0.478	0.635

Due to the nonlinear behaviour of the hydrological model, the description of this smaller flood is even worse than the corresponding hyetograph (fig. 10a,b). Since the runoff coefficient generally increases as the soil saturates during the storm, the underestimation of the flow is not proportional to that of the rainfall. Forecasts 1 (not shown) and 3 (fig. 10b) show a marked underestimate of the peak due to the difference between the rain-gauge estimate and the LAM prediction of the total depth. Forecast 2 (fig. 10a) gives a good forecast exactly for the same reasons as for the preceding events.

Case 4: December 13-14, 1996 – Neither is this event not associated with a marked synoptic scale meteorological situation. This explains why the ECMWF model is unable to adequately describe the phenomenon, both in rain volumes and in time structure (fig. 11a). As in the previous case, the LAM provides a better performance in terms of time-structure of the event (fig. 11b and table IV).

As what concerns the flood, the same considerations apply as to the previous event. Figure 12a,b shows the forecasts 2 and 3, while forecast 1 is not shown.

It is worth noting that the strong difference in total rainfall volumes between ground observations and meteorological forecasts yield substantial underestimates of surface flows. This clearly appears in forecasts 1 and 3. In forecast 2, flood predictions are quite close to the observed discharges. Due to the response-time of the basin and to the length of the storm, a 24 h lead time in forecasting implies that the precipitation which feeds the direct overland flow has already fallen when the forecast is delivered.

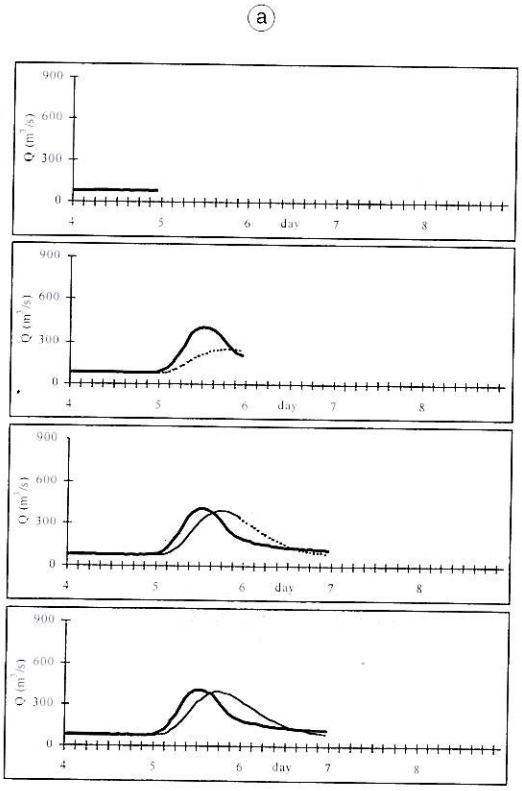

Fig. 10a,b. Case 3, January 1994. Flood forecasting sequence: a) forecast 2, 24-h forecast using LAM rainfall forecast only for the last 24 h: thick line refers to the observed flow, thin line refers to the first part of the forecast and dotted line refers to the second part of the forecast (last 24 h); b) forecast 3, 48-h forecast using LAM rainfall forecast: thick line refers to the observed flow, dotted line refers to the forecast flow. The last hydrograph represents the comparison between observed (thick line) and modelled (thin line) flood flows using calibration rainfall data as input to the hydrological model.

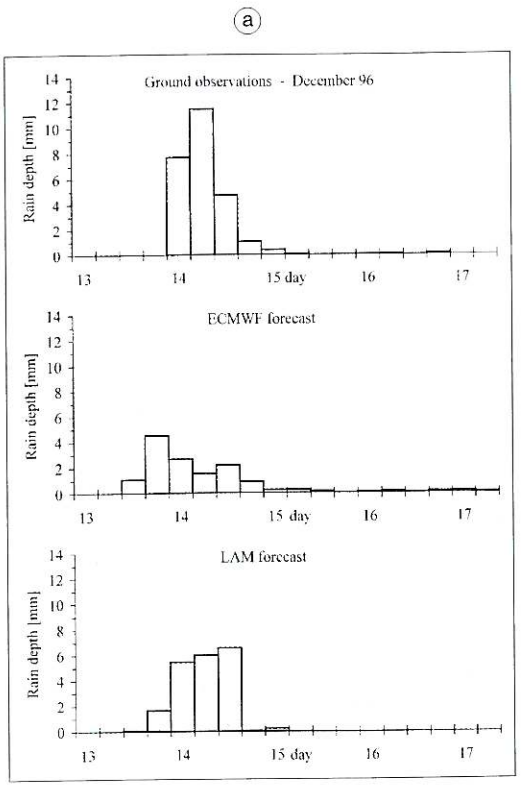

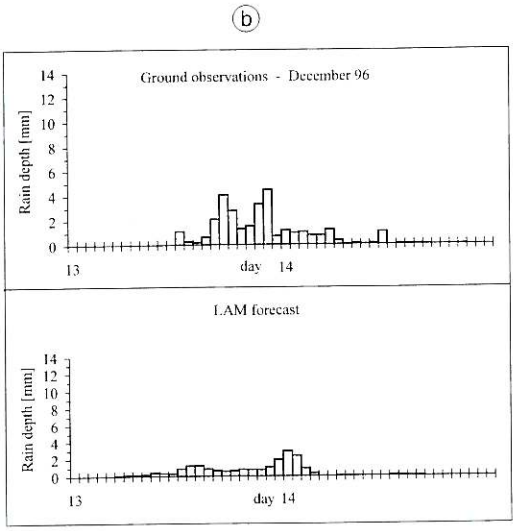

Fig. 11a,b. As fig. 9a,b, but for Case 4, December 1996.

Table IV. As table III, but for Case 4, December 1996.

December 1996	TD (mm)	TD_{Ratio}	PI (mm)	PI_{Ratio}	SE
Obs. - 6 h	25.3	–	11.5	–	–
ECMWF	13.4	0.528	4.5	0.393	2.772
LAM - 6 h	20.0	0.791	6.6	0.571	3.244
Obs. - 1 h	*	–	4.4	–	–
LAM - 1 h	*	*	2.9	0.656	1.021

4. Conclusions

From the comparative analysis of the limited number of case studies considered we tentatively conclude that:

– The time evolution of the precipitation field over the basin is adequately forecast.

– The definition of the above time evolution improves with the numerical resolution.

But:

– Forecasts show a systematic deficit of precipitated water.

– The precipitation deficit is neither removed, nor mitigated by the improvement in numerical resolution.

For our purposes of service operation, the results of this preliminary study seemed to be encouraging. More in-depth studies are required,

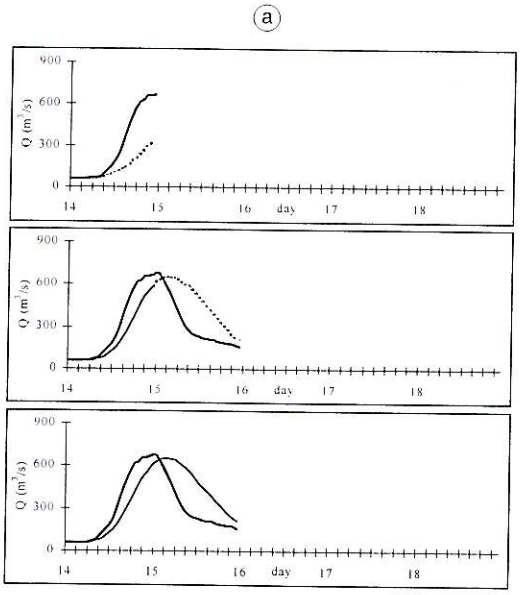

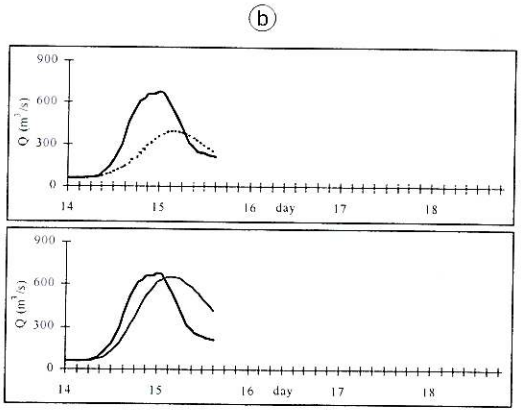

Fig. 12a,b. As fig. 10a,b, but for Case 4, December 1996.

in particular as concerns the causes of the LAM precipitation underestimation, if this is confirmed by further numerical experiments.

Acknowledgements

The authors thank the «Dipartimento dei Servizi Tecnici Nazionali» of the Italian «Presidenza del Consiglio dei Ministri» for the support given to this study.

REFERENCES

BRENT, R.P. (1973): *Algorithms for Minimization Without Derivatives* (Prentice-Hall, Englewood Cliffs, NJ), pp. 232.

BUZZI, A., M. FANTINI, P. MALGUZZI and F. NEROZZI (1994): Validation of a limited area model in case of Mediterranean cyclogenesis: surface fields and preciptation scores, *Meteorol. Atmos. Phys.*, **36**, 91-107.

COURTIER, P., E. ANDERSSON, W. HECKLEY, J. PALLIEUX, D. VASILJEVIC, M. HAMRUD, A. HOLLINGSWORTH, F. RABIER and M. FISHER (1998): The ECMWF implementation of three-dimensional variational assimilation (3D-Var). Part I: formulation, *QJR. Meteorol. Soc.*, **124**, 1783-1807.

DALEY, R. (1991): *Atmospheric Data Analysis*, in Cambridge Atmospheric and Space Sciences Series (Cambridge University Press), pp. 457.

EMANUEL, K. (1991): A scheme for representing cumulus convection in large-scale models, *J. Atmos. Sci.*, **48**, 2313-2335.

GELEYN, J.F and A. HOLLINGSWORTH (1979): An economical analytical method for the computation of the interaction between scattered and line absorbption of radiation, *Contrib. Atmos. Phys.*, **52**, 1-16.

HOLTON, J.R. (1992): *An Introduction to Dynamic Meteorology* (Academic Press), pp. 511.

LORENC, A.C. (1981): A global three-dimensional multivariate statistical interpolation scheme, *Mon. Weather Rev.*, **109**, 701-721.

LOUIS, J.F., M. TIEDKE and J.F. GELEYN (1982): A short history of the PBL parameterization at ECMWF, in *Proceedings of ECMWF Workshop on PBL Parameterization, Reading 25-27 November 1981*, 59-80.

NASH, J.E. (1957): *The Form of the Instantaneous Unit Hydrograph* (IASH publication), No. 45, vol. 3-4, 121-141.

NATALE, C. and E. TODINI (1977): A constrained parameter estimation technique for linear model in hydrology, in *Mathematical Model for Surface Water Hydrology*, edited by A. CIRIANI, U. MAIONE and G.R. WALLIS (Elsevier), 108-147.

U.K. METEOROLOGICAL OFFICE (1962): *Weather in the Mediterranean* (Her Majesty's Stationery Office, London), pp. 261.

(received September 15, 1999;
accepted June 5, 2000)

Appendix I. Meteorological models and data.

A simple outline of the ECMWF model and data assimilation scheme is given, for example, in § 13.6 and § 13.7 of Holton's book (Holton, 1992) respectively. A comprehensive exposition of analysis and assimilation issues can be found, for example, in Daley (1991).

ECMWF analysis is obtained from a large set of observations, including SYNOP land-based observations, rawinsondes, observations from ship and airplanes, and satellite data. These are provided in real-time to the ECMWF through the Global Telecommunication System (GTS).

Assimilation is the operation which produces a regularly-gridded analysis from the data, which are extremely sparse and non-homogeneous. This can be done in many different ways. Until January 1996, an Optimal Interpolation (OI) algorithm was used (Lorenc, 1981). It produces corrections to a background field (a previous forecast) as a weighted spatial average of observations, and incorporates the information about physical relationships between the variables by means of statistical information about departure of analysis from background field (error covariance matrices). Hereafter, a variational algorithm or 3D-Var (Courtier *et al.*, 1998) was implemented: the problem is rewritten as the minimization of a cost function which is derived from the model equations, so that observed data are «assimilated» in a frame coherent with the model. This approach is able to assimilate any kind of observation at a given instant. The space-time extension of this algoritm, the 4D-Var, is currently operating at ECMWF. All observation, analysis and forecast data are stored in the Centre's archive system and are available as a facility to the Member States' scientific community.

The ECMWF global forecast model is (currently) a semi-Lagrangian global spectral primitive equation model, with resolution about 50 km at mid-latitude and 40 vertical (sigma) levels. The model is continuously improved, so its technical characteristics vary in time.

Twice a day (at 00 and 12 UTC) a forecast run, initialised with current analysis, is performed up to 10 days of forecast time.

In this study we use a version of a grid-point, hydrostatic, primitive-equations LAM, commonly known as BOLAM (Buzzi *et al.*, 1994).

Prognostic variables (horizontal wind, ground-level pressure, potential temperature and specific humidity) are defined over a sigma-coordinate, staggered grid (Arakawa-Lamb C grid) and are updated by a semi-implicit «leapfrog» time integration scheme. Horizontal diffusion is introduced to avoid numerical instability. Horizontal divergence diffusion is also included, in order to damp spurious gravity-wave growth.

Horizontal resolution is 27.5 km and 20 vertical terrain-following levels (sigma levels) are used. The model grid covers a 3300 km (long.) $\times$ 2700 km (lat.) area, centered in the position of coordinates 12.5°E, 45.0°N.

The model uses initial and boundary values of the model prognostic variables, as obtained from the ECMWF 0.5 degree analysis fields; these need to be pre-processed before being input into the model. The boundary conditions are imposed every time-step by means of a relaxation scheme over the horizontal boundaries of the grid. Other input (static) fields are the mean orographic elevation and the land-sea mask (percentage area covered by land) of the surface grid-boxes. Several parameterization-schemes are included to account for the unresolved physical processes. Most of these parameterization-schemes are analogous to those of the ECMWF model (Louis *et al.*, 1982). Turbulent (numerically unresolved) fluxes of momentum, heat and moisture are represented according to similarity theories and depend on surface roughness and atmospheric static stability. For radiative energy fluxes, a parameterization scheme by Geleyn (Geleyn and Hollinsgworth, 1979) is used. Dry convective adjustment is used whenever static instability conditions occur. Soil is represented by a three-layer scheme accounting for heat and moisture diffusion in the ground down to a climatological (constant-value) layer. Snow occurrence is accounted for in heat and moisture surface-atmosphere exchange and albedo. Precipitation processes are represented in two ways: large-scale precipitation is simply computed by letting the exceeding vapour condensate and precipitate by means of a numerical relaxation-scheme; precipitating water can also re-evaporate in the lower layers; convective precipitation is described by an advanced parameterization scheme (Emanuel, 1991) which is fundamentally a bulk description of vertical currents and evaporation-condensation-precipitation processes inside the clouds. Finally, a post-processing module is used in order to convert forecast field on sigma-levels into a more conventional and suitable form.

Appendix II. The rainfall-runoff lumped model.

The hydrological model was developed by the authors within a broader research activity in the field of advanced hydrology modelling, carried out at the «Dipartimento di Scienza dell'Ingegneria Civile» of the University of «Roma Tre».

The model is based on hypothesis and algorithms widely discussed in the international literature and frequently utilised in research and operational applications.

The model is formed by three modules:

– A *base flow module*, accounting for the contributions of the subsurface flow.

– A *hydrological losses module*, accounting for losses due to evapotranspiration, interception, depression storage and infiltration.

– A *flow concentration module*, accounting for the overland flow and for the channel flow in the concentration process.

The *base flow* – Considering that the base flow is much lower than the flood flow, which is the objective of the forecast, the base flow is simply set equal to the river discharge at the beginning of the time of the forecast.

The *hydrological losses module* – The excess rainfall is calculated by a runoff coefficient, that is, as a fraction of total precipitation. The value of the runoff coefficient increases with rain depth following a double step algorithm as the depth exceeds fixed thresholds

$$I(t) = \phi_0 I_{tot}(t) \qquad I_{tot}(t) < T_1$$

$$I(t) = \phi_1 I_{tot}(t) \qquad T_1 < I_{tot}(t) < T_2$$

$$I(t) = \phi_3 I_{tot}(t) \qquad I_{tot}(t) > T_2.$$

The adopted methods follows a threshold approach well spread in research and application (see, for example, Natale and Todini, 1977).

The *flow concentration module* – A Nash model (Nash, 1957) has been used as flow concentration module. The Nash model is a conceptual model, formed by a cascade of linear reservoirs.

The solution of a linear model is given by the convolution equation

$$Q(t) = \int_0^t u(\tau) I(t-\tau) d\tau$$

where $u(\tau)$ is the instantaneous unit hydrograph of the selected model.

A linear reservoir is a schematised basin where the storage S is linearly related to the output discharge Q by the continuity equation

$$k \frac{dQ}{dt} = I(t) - Q(t)$$

where: $I(t)$ is the input to the reservoir, that is the spatialy integrated rain intensity over the basin, reduced by the runoff coefficient, for the first reservoir, and the output of the upstream reservoir for the other ones; k is the storage coefficient, constant for all the reservoirs.

The instantaneous unit hydrograph for a linear reservoir is

$$u(t) = \frac{1}{k} e^{-t/k}.$$

It follows that the instantaneous unit hydrograph for the Nash scheme is

$$u(t) = Q_n(t) = \frac{1}{k\Gamma(n)} \left(\frac{t}{k}\right) e^{-t/k}.$$

The overall hydrologic model is characterised by 7 parameters ϕ_1, ϕ_2, ϕ_3, T_1, T_2, n, k.

The calibration procedure for determining the parameter values from the available data involves the minimisation of the following objective function:

$$F = \sqrt{\frac{\sum (Q_{oss} - Q_{sim})^2}{\sum Q_{oss}^2}}.$$

Powell's conjugate directions method (Brent, 1973) has been used as minimisation algorithm.